

# Electroweak Physics at the Tevatron and LHC: Theoretical Status and Perspectives

Ulrich Baur

Physics Department, State University of New York at Buffalo, Buffalo, NY 14260, USA

Received: date / Revised version: date

**Abstract.** I review the status of theoretical calculations relevant for electroweak physics at the Tevatron and LHC and discuss future directions. I also give a brief overview of current electroweak data and discuss future expectations.

**PACS.** PACS-key describing text of that key – PACS-key describing text of that key

## 1 Introduction

Electroweak measurements are a very important part of the physics program of the Tevatron and the LHC. Of particular interest are the search for the Higgs boson and the determination of its properties, and the measurement of electroweak precision observables, in particular the measurement of

- the  $W$  mass,  $M_W$ , and  $W$  width,  $\Gamma_W$ ,
- the effective weak mixing angle,  $\sin^2 \theta_{eff}$ , and the forward – backward asymmetry,  $A_{FB}$ ,
- the  $W$  and  $Z$  boson cross sections,  $\sigma(W)$  and  $\sigma(Z)$ , and their ratio,  $R_{W/Z}$ ,
- the  $W$  forward backward charge asymmetry,  $A(\eta_e)$ ,
- the  $\ell^+ \ell^- (\ell\nu)$  differential cross sections above the  $Z$  ( $W$ ) peak,
- and di-boson ( $W\gamma$ ,  $Z\gamma$ ,  $WW$ ,  $WZ$  and  $ZZ$ ) production.

In the following I discuss the physics interest in these measurements, give a brief overview of the current experimental status and what to expect in the future (for more details see Refs. [1] – [3]), and discuss the current status and the prospects of the relevant theoretical calculations.

## 2 Weak Boson Physics

### 2.1 Measurement of the $W$ mass

The one-loop corrections to  $M_W$  depend quadratically on the top quark mass,  $m_t$ , and logarithmically on the Higgs boson mass,  $m_H$ . Precise measurements of  $M_W$  and  $m_t$  thus make it possible to extract information on  $m_H$ .

Send offprint requests to:

In Run I of the Tevatron, the  $W$  mass has been measured to  $M_W = 80.456 \pm 0.059$  GeV [4]. The preliminary value of the  $W$  mass from LEP2 is  $M_W = 80.392 \pm 0.039$  GeV [5]. When combined with the current world average of the top quark mass,  $m_t = 172.7 \pm 2.9$  GeV [6], this yields  $m_H < 219$  GeV at 95% CL [5] for a Standard Model (SM) Higgs boson.

In Run II, one hopes to achieve a precision of  $\delta M_W = 40$  MeV per lepton channel and experiment for an integrated luminosity of  $2 \text{ fb}^{-1}$  [7], while the LHC may be able to reach a precision of  $\delta M_W \approx 10$  MeV using the  $W/Z$  transverse mass ratio and  $W \rightarrow \mu\nu$  decays [8]. The present constraints on  $M_W$  and  $m_t$  from LEP2 and Tevatron data, and the results expected from measurements at the LHC, are compared with theoretical predictions in Fig. 1. Present data clearly favor a light SM Higgs boson, and are also in very good agreement with predictions of the minimal supersymmetric standard model (MSSM) [9].

To ensure that the  $M_W$  and  $m_t$  measurements contribute equally to the uncertainty in a  $\chi^2$  test, the precision on the top quark mass and the  $W$  mass should satisfy the relation [10]

$$\delta M_W \approx 7 \times 10^{-3} \delta m_t. \quad (1)$$

Since one expects to measure the top quark mass with a precision of  $\delta m_t = 1 - 2$  GeV at the LHC [11], one needs to determine the  $W$  mass with a precision of about  $\delta M_W \approx 10$  MeV so that it does not become the dominant uncertainty in the estimate of  $m_H$ . Accurate theoretical predictions for  $W$  production are absolutely essential in order to measure the  $W$  mass with a precision of 10 MeV.

### 2.2 $\sin^2 \theta_{eff}$

Constraints on  $m_H$  can also be derived from the top quark mass and the effective weak mixing angle. At LEP, the ef-

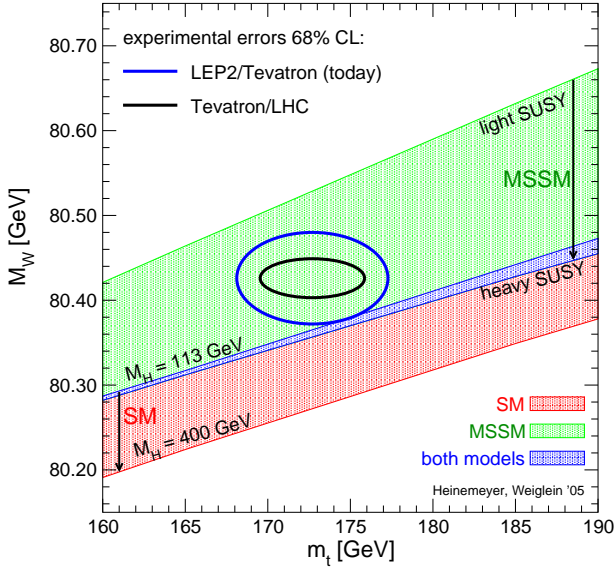


**Fig. 1.** Constraints on  $M_W$  and  $m_t$  from LEP2 and Tevatron data, and expectations from the LHC, compared with the predictions of the SM and the MSSM.

fective weak mixing angle has been measured to  $\sin^2 \theta_{eff} = 0.23153 \pm 0.00016$  [12]. This will be difficult to improve at the Tevatron or LHC. From a measurement of the forward – backward asymmetry,  $A_{FB}$ , at the Tevatron one expects to reach a precision of  $\delta \sin^2 \theta_{eff} = 0.0006$  per lepton channel and experiment for an integrated luminosity of  $10 \text{ fb}^{-1}$  [7]. At the LHC, with  $100 \text{ fb}^{-1}$ , one hopes to achieve  $\delta \sin^2 \theta_{eff} = 0.00014$  using forward electrons in a measurement of  $A_{FB}$  in  $Z \rightarrow e^+e^-$  events [13].

### 2.3 The Weak Boson Cross Sections and the $W/Z$ Cross Section Ratio

In the past, the measurement of the  $W$  and  $Z$  boson cross sections has provided a test of perturbative QCD. With the large data sets of Run II and the LHC, non-statistical uncertainties, in particular the luminosity error, become limiting factors. This is illustrated by the recent  $D\bar{O}$  measurements of the  $W$  and  $Z$  production cross sections [14]

$$\begin{aligned} \sigma(W) \cdot B(W \rightarrow e\nu) &= 2865.2 \pm 8.3(\text{stat}) \pm 62.8(\text{sys}) \\ &\quad \pm 40.4(\text{pdf}) \pm 186.2(\text{lumi}) \text{ pb}, \\ \sigma(Z) \cdot B(Z \rightarrow e^+e^-) &= 264.9 \pm 3.9(\text{stat}) \pm 8.5(\text{sys}) \\ &\quad \pm 5.1(\text{pdf}) \pm 17.2(\text{lumi}) \text{ pb}. \end{aligned}$$

Provided that the  $W$  and  $Z$  cross sections are accurately predicted by theory, and the PDF uncertainties can be controlled,  $\sigma(W)$  and  $\sigma(Z)$  can be used as luminosity monitors.

The cross section ratio

$$R_{W/Z} = \frac{\sigma(p\bar{p} \rightarrow W \rightarrow \ell\nu X)}{\sigma(p\bar{p} \rightarrow Z \rightarrow \ell^+\ell^- X)}, \quad (2)$$

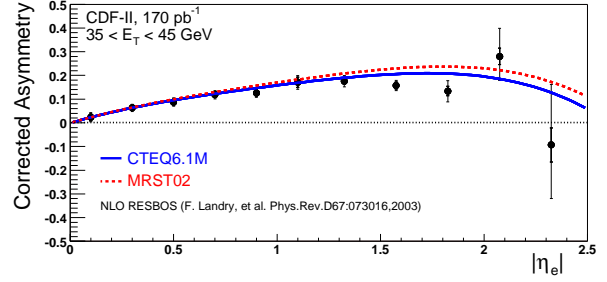


**Fig. 2.** The  $W$  charge asymmetry as a function of  $\eta_e$  for electrons with  $35 \text{ GeV} < E_T < 45 \text{ GeV}$  and two different PDF parametrizations.

together with the theoretical prediction for the ratio of the total  $W$  and  $Z$  production cross sections, the LEP measurement of the branching ratio  $B(Z \rightarrow \ell^+\ell^-)$ , and the SM prediction for the  $W \rightarrow \ell\nu$  decay width, can be used for an indirect determination of  $\Gamma_W$ . A recent CDF measurement,  $\Gamma_W = 2079 \pm 41 \text{ MeV}$  [15], is in good agreement with the SM prediction  $\Gamma_W^{SM} = 2092 \pm 3 \text{ MeV}$  [16].

### 2.4 Direct Measurement of $\Gamma_W$

The width of the  $W$  boson can also be measured directly from the tail of the  $W \rightarrow \ell\nu$  ( $\ell = e, \mu$ ) transverse mass ( $M_T$ ) distribution. Unlike the extraction of  $\Gamma_W$  from  $R_{W/Z}$ , the measurement from the tail of the  $M_T$  distribution does not depend on theoretical assumptions; however, the method is currently not as precise as the measurement using  $R_{W/Z}$ . This is illustrated by the recent combined Tevatron result,  $\Gamma_W = 2078 \pm 62(\text{stat}) \pm 60(\text{syst}) \text{ MeV}$  [17]. For  $2 \text{ fb}^{-1}$  one expects the direct measurement of  $\Gamma_W$  to improve to  $\delta\Gamma_W = 50 \text{ MeV}$  per lepton channel and experiment [18].

### 2.5 The $W$ charge asymmetry

Another important electroweak measurement is that of the  $W$  charge asymmetry,

$$A(\eta_e) = \frac{d\sigma(e^+)/d\eta_e - d\sigma(e^-)/d\eta_e}{d\sigma(e^+)/d\eta_e + d\sigma(e^-)/d\eta_e}, \quad (3)$$

where  $\eta_e$  is the rapidity of the electron in  $W \rightarrow e\nu$ .  $A(\eta_e)$  is sensitive to the  $u$ - and  $d$ -quark components of the PDFs, especially at large values of  $\eta_e$  and the electron transverse energy,  $E_T$ . Results from CDF for  $170 \text{ pb}^{-1}$  of Run II data [19] are shown in Fig. 2.

### 2.6 Search for New Physics in Drell-Yan Production

Many models of new physics predict new charged ( $W'$ ) or neutral ( $Z'$ ) gauge bosons. One can search for these particles in the high  $\ell^+\ell^-$  ( $\ell\nu$ ) invariant (transverse) mass region. Information on the couplings of a  $Z'$  boson can be

obtained from the forward – backward asymmetry,  $A_{FB}$ , at large di-lepton masses. Present  $D\bar{O}$  data ( $200 \text{ pb}^{-1}$ ) require that  $m_{Z'} > 780 \text{ GeV}$  at 95% CL for a SM-like  $Z'$  boson [20].

At the LHC, one can discover a  $Z'$  boson with  $m_{Z'} = 4 - 5 \text{ TeV}$  for  $300 \text{ fb}^{-1}$  and one will be able to severely constrain the couplings of the new vector boson [21].

## 2.7 Theory of Single Weak Boson Production

The precision foreseen for electroweak measurements in Run II and at the LHC has to be matched by precise theoretical predictions, ie. QCD and electroweak (EW) radiative corrections have to be under control.

The QCD corrections to the total  $W$  and  $Z$  boson cross sections at the next-to-next-to-leading (NNLO) level have been known for more than a decade [22]. Recently, the rapidity distribution of the  $Z$  boson has been calculated at NNLO, showing a dramatically reduced dependence of the differential cross section on the unphysical renormalization and factorization scales compared with the NLO prediction [23]. Calculations of the resummed QCD corrections to predict the transverse momentum ( $q_T$ ) distributions of the  $W$  and  $Z$  bosons are also available [24]. The precise shape of the weak boson  $q_T$  distribution for small transverse momenta, however, is still uncertain, in particular at the LHC [25].

With the the uncertainty from unknown higher order QCD corrections approaching the 1% level [23], EW radiative corrections to weak boson production become important. EW corrections may also be enhanced by collinear logarithms near the  $W$  and  $Z$  resonances, and by Sudakov logarithms at large  $\ell^+\ell^-$  and  $\ell\nu$  invariant masses. A consistent calculation of EW radiative corrections requires parton distribution functions (PDFs) which take into account QED corrections. Such PDFs exist now [26].

There has been significant progress in the calculation of the EW radiative corrections to  $W$  and  $Z$  boson production in the past few years. Calculations of the full  $\mathcal{O}(\alpha)$  EW corrections are available now [27, 28].

The main effect of the EW corrections in the vicinity of the  $W$  and  $Z$  resonances is that they shift the  $W$  and  $Z$  masses extracted from data. The magnitude of the shift is about 50 MeV (150 MeV) for  $W \rightarrow e\nu$  ( $W \rightarrow \mu\nu$ ). Since both leptons can radiate photons, the shifts are about twice as large in  $Z$  events. The shift is mostly caused by final state photon radiation which is enhanced due to collinear logarithms of the form  $(\alpha/\pi) \log(M_{W,Z}^2/m_\ell^2)$ , where  $m_\ell$  is the mass of the charged lepton in  $W \rightarrow \ell\nu$  or  $Z \rightarrow \ell^+\ell^-$ . Final state photon radiation distorts the shape of the Breit-Wigner resonance by reducing the peak cross section by 20 – 30%, and (significantly) enhancing the cross section below the peak. This is shown in Fig. 3 for the  $Z$  case with only QED corrections taken into account [29].

Above the  $W/Z$  peak, the purely weak corrections become increasingly important, due to Sudakov-like logarithms of the form  $(\alpha/\pi) \log^2(\hat{s}/M_{W,Z}^2)$ , where  $\hat{s}$  is the

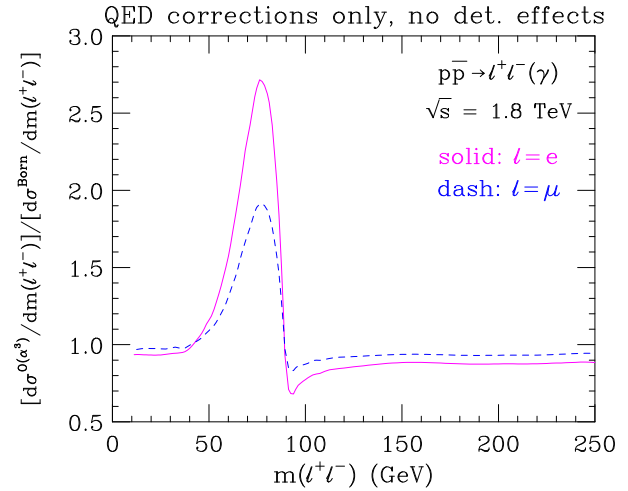


**Fig. 3.** Ratio of the  $\mathcal{O}(\alpha^3)$  and lowest order differential cross sections as a function of the di-lepton invariant mass for  $p\bar{p} \rightarrow \ell^+\ell^-(\gamma)$  at  $\sqrt{s} = 1.8 \text{ TeV}$ .

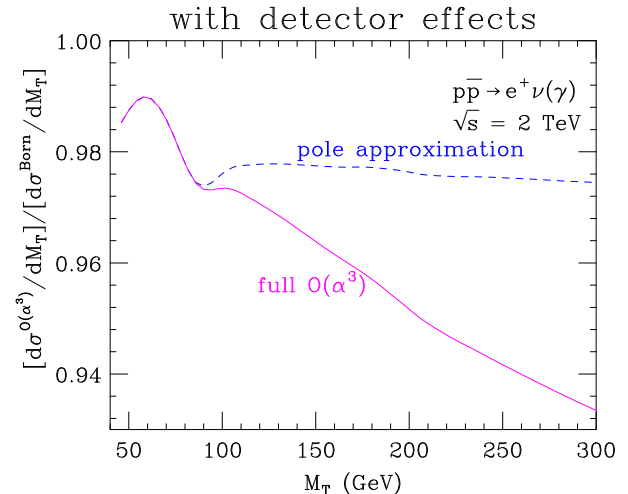


**Fig. 4.** The ratio  $[d\sigma^{\mathcal{O}(\alpha^3)}/dM_T]/[d\sigma^{\text{Born}}/dM_T]$  as a function of the transverse mass for  $p\bar{p} \rightarrow e^+\nu_e(\gamma)$  at  $\sqrt{s} = 2 \text{ TeV}$ .

squared invariant mass of the  $\ell^+\ell^-$  or  $\ell\nu$  system. This is shown in Fig. 4 for the  $e\nu$  transverse mass. The solid line shows the ratio  $[d\sigma^{\mathcal{O}(\alpha^3)}/dM_T]/[d\sigma^{\text{Born}}/dM_T]$  taking into account the complete  $\mathcal{O}(\alpha)$  EW corrections. The dashed line shows the ratio in the pole approximation [27, 28] where the  $WZ$  box diagrams responsible for the Sudakov logarithms are absent.

Since the logarithmic terms from the  $WZ$  box diagrams change the slope of the  $M_T$  distribution, they shift the  $W$  width extracted from the tail of the  $M_T$  distribution. This shift,  $\delta\Gamma_W \approx -7 \text{ MeV}$  [27], while not large, cannot be neglected if the Run II goal (see Sec. 2.4) should be met.

At the LHC, it will be possible to probe di-lepton invariant and  $\ell\nu$  transverse masses of several TeV. In this region, the Sudakov logarithmic terms grow so large that

they have to be resummed. Although the resummation of electroweak Sudakov-like logarithms in general four fermion electroweak processes has been discussed in the literature [30,31], a calculation of  $\ell\nu$  production in hadronic collisions which includes resummation of electroweak logarithms has not been carried out yet.

Since final state photon radiation causes a significant shift in  $M_W$  and  $M_Z$ , one has to worry about multiple (final) state photon radiation in weak boson production. Two photon radiation is known to considerably change the shape of the dilepton and  $\ell\nu$  transverse mass distributions [32]. Recently, there have been several calculations of multi-photon radiation in  $W$  [33,34] and  $Z$  decays [35]. The shift in the weak boson masses caused by multiple photon radiation is found to be about 10% of the shift originating from one-photon emission [34,35]. For the muon final state, where the shift in the weak boson masses is particularly large, this is a non-negligible effect.

The experimental precision which can be achieved for  $M_W$  strongly depends on how well the transverse momentum distribution of the  $W$  is known. Knowledge of the  $W$   $q_T$  distribution determines the missing transverse energy ( $\cancel{E}_T$ ) resolution in  $W$  events. The  $\cancel{E}_T$  resolution determines how “sharp” the edge in the  $M_T$  distribution at  $M_T \approx M_W$  is, which in turn determines how well  $M_W$  can be measured. To constrain the  $W$   $q_T$  distribution, one uses data on the transverse momentum distribution of the  $Z$  boson, together with a theoretical prediction for the ratio  $[\frac{d\sigma(W)}{dq_T(W)}]/[\frac{d\sigma(Z)}{dq_T(Z)}]$ . For the  $W$  mass measurement one thus needs a calculation which includes both the resummed QCD corrections, the full  $\mathcal{O}(\alpha)$  EW corrections, and effects from multiple photon radiation. A first step towards this lofty goal has been taken in Ref. [36], where final state photon radiation was added to a calculation of  $W$  boson production which includes resummed QCD corrections.

## 3 Di-boson Production

### 3.1 Experimental Results

Di-boson production makes it possible to probe the  $WW\gamma$ ,  $WWZ$ ,  $Z\gamma\gamma$ ,  $ZZ\gamma$  and  $ZZZ$  self-couplings (TGCs). For details on these couplings and recent TGC measurements at the Tevatron see Ref. [3]. In the following I concentrate on the  $WW\gamma$  and  $WWZ$  couplings and briefly summarize recent experimental results for these couplings.

The most general  $WWV$  ( $V = \gamma, Z$ ) vertex consistent with Lorentz invariance and electromagnetic gauge invariance has seven free parameters [37]. Assuming  $C$  and  $P$  conservation, five independent couplings,  $g_1^Z$ ,  $\kappa_V$  and  $\lambda_V$ , remain. Requiring SU(2) invariance as well,  $\lambda_Z = \lambda_\gamma$  and  $\kappa_Z = g_1^Z - (\kappa_\gamma - 1) \tan^2 \theta_W$ , where  $\theta_W$  is the weak mixing angle [38], and one is left with three independent couplings. In the SM, at tree level,  $g_1^Z = \kappa_V = 1$  and  $\lambda_V = 0$ . In order to avoid that  $S$ -matrix unitarity is violated, deviations of the TGCs from their SM values have to be momentum dependent form factors which depend on the

form factor scale,  $\Lambda$  [39]. The form factor scale is related to the scale of the new physics which causes non-SM TGCs.

The  $WWV$  couplings can be measured in  $e^+e^- \rightarrow W^+W^-$ , and in  $W\gamma$ ,  $WZ$  and  $WW$  pair production at hadron colliders. Assuming  $C$ ,  $P$  and SU(2) invariance, the LEP experiments have determined the independent couplings to [40]

$$\begin{aligned} g_1^Z &= 0.984_{-0.019}^{+0.022}, \\ \kappa_\gamma &= 0.973_{-0.045}^{+0.044}, \\ \lambda_\gamma &= -0.028_{-0.021}^{+0.020}. \end{aligned}$$

$W^+W^-$  production is sensitive to both the  $WW\gamma$  and the  $WWZ$  couplings. To measure these couplings independently, one has to consider  $W\gamma$  and  $WZ$  production in hadronic collisions. Measurements of the  $WW\gamma$  couplings in  $W\gamma$  production have been performed in Run I [41] and in Run II [3]. The DØ Collaboration recently presented the first direct measurement of the  $WWZ$  couplings from  $WZ$  production. For  $0.3 \text{ fb}^{-1}$ , and assuming  $\Lambda = 1.5 \text{ TeV}$ , they found that [42]

$$\begin{aligned} -0.48 < \lambda_Z < 0.48 & \quad \text{for } \kappa_Z = g_1^Z = 1, \\ 0.51 < g_1^Z < 1.66 & \quad \text{for } \lambda_Z = \kappa_Z - 1 = 0 \end{aligned}$$

at 95% CL. Note that, at hadron colliders, TGC limits depend on the form factor scale,  $\Lambda$ .

Bounds on TGCs from hadron collider experiments scale roughly with  $(\int \mathcal{L} dt)^{1/4}$ . One thus expects that the ultimate precision which can be reached for the  $WWV$  couplings at the Tevatron will be a factor 1.6 to 2.5 better than that obtained from current data, depending on the final integrated luminosity. While the TGC bounds at the Tevatron only mildly depend on the form factor scale, the dependence on  $\Lambda$  is much more pronounced at the LHC. In general, the  $WWV$  couplings can be measured with a precision of  $\mathcal{O}(10^{-2} - 10^{-3})$  at the LHC [10].

### 3.2 Theory of Di-boson Production

All di-boson production processes are known to NLO in QCD [43]. At the LHC QCD corrections to di-boson production are large and increase with the  $p_T$  of the vector bosons. The ratio of the NLO to LO cross sections ( $k$ -factor) for  $W^+Z$  production at the LHC as a function of  $p_T(Z)$  is shown in Fig. 5. Qualitatively similar results are obtained for the other di-boson processes. Since the QCD corrections give an effect which is qualitatively similar to that of anomalous TGCs, it will be essential to take them into account in any LHC di-boson analysis.

The EW radiative corrections to the di-boson production processes are also known [44]. As in the case of single weak boson production, they become significant at large energies, due to EW Sudakov logarithms. For invariant masses in the TeV region they reduce the cross section by typically 5 – 20%.

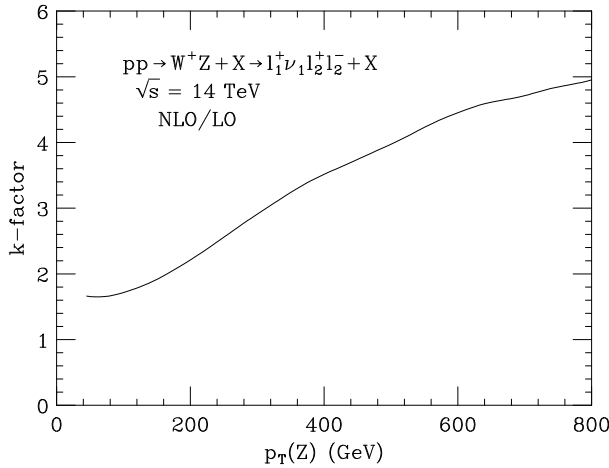


**Fig. 5.** The ratio of the NLO to LO cross sections as a function of  $p_T(Z)$  for  $W^+Z$  production at the LHC.

## 4 Higgs Boson Physics

The search for the SM Higgs boson is one of the main objectives of the LHC. Over the last decade, enormous progress has been made in providing accurate predictions for Higgs boson production and decays. In addition, in the last few years, many studies of how well the Higgs properties can be determined once this particle has been found have been performed.

The NLO QCD corrections to Higgs production via gluon fusion have been calculated more than 10 years ago [45]. They enhance the  $gg \rightarrow H$  cross section by a factor 1.5 – 2. More recently, several groups have calculated the NNLO QCD corrections to the total  $gg \rightarrow H$  cross section in the  $m_t \rightarrow \infty$  limit [46], showing that the perturbative series starts to converge at this order. A fully differential NNLO calculation for  $gg \rightarrow H \rightarrow \gamma\gamma$  also exists [47]. Finally, the  $\mathcal{O}(\alpha)$  corrections to Higgs production via gluon fusion have been computed [48]. They change the Higgs production cross section by 5 – 8% if  $m_H = 115 - 160$  GeV.

For  $m_H < 200$  GeV, production via vector boson fusion (VBF),  $qq' \rightarrow Hqq'$ , is an important source for Higgs bosons. The QCD corrections to  $qq' \rightarrow Hqq'$  have been found to be modest [49]. Associated production of Higgs bosons and top quarks,  $pp \rightarrow t\bar{t}H$ , is a tool for measuring the top quark Yukawa coupling. At LO, the  $t\bar{t}H$  cross section strongly depends on the factorization and renormalization scales. Once NLO QCD corrections are taken into account, this dependence is greatly reduced [50].

While Higgs production is well under control theoretically, more reliable calculations are still needed for several background processes. In particular, calculations of the NLO QCD corrections are needed for  $t\bar{t}j$ ,  $t\bar{t}b\bar{b}$  and EW  $WWjj$  production.

Once a Higgs candidate has been found, one would like to determine how the new particle couples to fermions, gauge bosons, and to itself. Several studies have shown that, with mild theoretical assumptions, the couplings of

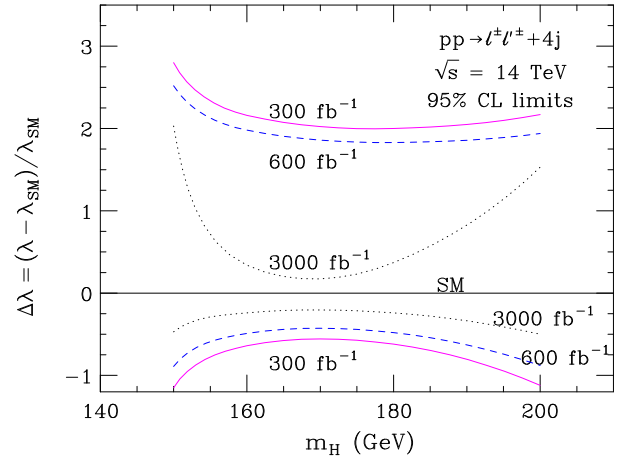


**Fig. 6.** Limits achievable at 95% CL for the normalized Higgs boson self-coupling,  $\Delta\lambda_{HHH} = (\lambda - \lambda_{SM})/\lambda_{SM}$ , at the LHC.

the new particle to fermions and gauge bosons can be measured with a precision of 10 – 30% at the LHC [51].

A measurement of the three Higgs boson self-coupling,  $\lambda$ , with a similar precision is considerably more difficult. In order to probe  $\lambda$ , one has to study Higgs pair production,  $gg \rightarrow HH$ . For  $m_H \geq 150$  GeV, the  $HH \rightarrow 4W \rightarrow \ell^\pm \ell'^\pm + 4j$  channel offers the best chances [52, 53]. As shown in Fig. 6, with  $300 \text{ fb}^{-1}$ , it may be possible to rule out a vanishing of  $\lambda$  for  $m_H = 150 - 200$  GeV, and measure the  $HHH$  coupling with up to 20% accuracy at a SuperLHC with  $3 \text{ ab}^{-1}$ . For  $m_H \leq 140$  GeV,  $HH \rightarrow b\bar{b}\gamma\gamma$  is the most promising final state. However, due to the tiny signal cross section in this channel, a luminosity upgrade for the LHC is needed. Even with  $3 \text{ ab}^{-1}$  one can only hope to achieve a precision of about 70% for  $\lambda$  [54].

While the signal to background ratio is of  $\mathcal{O}(1)$  for  $HH \rightarrow b\bar{b}\gamma\gamma$ , it is roughly  $1/5 - 1/10$  for the  $\ell^\pm \ell'^\pm + 4j$  final state. The largest backgrounds contributing to  $\ell^\pm \ell'^\pm + 4j$  production originate from  $WWWjj$ ,  $t\bar{t}W$  and  $t\bar{t}j$  production. The  $t\bar{t}j$  background is particularly sensitive to the acceptance cuts imposed, and thus tricky to estimate. More realistic simulations for this background are needed. Furthermore, both signal and background cross sections show a significant scale dependence which could be reduced by full calculations of the NLO QCD corrections to  $gg \rightarrow HH$  (for finite  $m_t$ ), and the background reactions. None of these exist at the moment.

## 5 Summary

Electroweak physics at hadron colliders is precision physics. Accurate predictions are needed to fully utilize the potential of the Tevatron and LHC for electroweak measurements. The theoretical predictions for weak boson and Higgs boson production have become increasingly accurate over the past few years. However, there is still much to do. In particular a calculation which combines QCD and EW radiative corrections for  $W$  and  $Z$  is needed, as well

as calculations of the NLO QCD corrections to a number of processes which contribute to the background in Higgs production.

## Acknowledgments

This research was supported by the National Science Foundation under grant No. PHY-0139953.

## References

1. S. Protopopescu, these proceedings.
2. M. Lancaster, these proceedings.
3. A. Goshaw, these proceedings.
4. V. M. Abazov *et al.* [CDF and DØ Collaborations], Phys. Rev. D **70** (2004) 092008.
5. M. Grünewald, talk given at the EPS2005 conference, Lisbon, Portugal, July 2005; C. Diaconu, arXiv:hep-ex/0510035.
6. The CDF and DØ Collaborations, arXiv:hep-ex/0507091.
7. R. Brock *et al.*, arXiv:hep-ex/0011009.
8. A. Schmidt, Diplomarbeit, Universität Karlsruhe, Germany, 2004; F. Gianotti, ATLAS-PHYS-99-001.
9. S. Heinemeyer and G. Weiglein, arXiv:hep-ph/0012364; A. Djouadi *et al.*, Phys. Rev. Lett. **78** (1997) 3626; Phys. Rev. D **57** (1998) 4179; S. Heinemeyer and G. Weiglein, JHEP **0210** (2002) 072.
10. S. Haywood *et al.*, arXiv:hep-ph/0003275.
11. M. Beneke *et al.*, arXiv:hep-ph/0003033.
12. S. Schael *et al.* [The ALEPH, DELPHI, L3, OPAL and SLD Collaborations], arXiv:hep-ex/0509008.
13. K. Sliwa, S. Riley, and U. Baur, ATLAS-PHYS-2000-018.
14. The DØ Collaboration, DØnote 4403-Conf (2004).
15. A. Abulencia *et al.* [CDF Collaboration], arXiv:hep-ex/0508029.
16. K. Hagiwara *et al.* [Particle Data Group], Phys. Rev. D **66** (2002) 010001.
17. B. Ashmankas *et al.* [Tevatron Electroweak Working Group], arXiv:hep-ex/0510077.
18. D. Amidei *et al.* [TeV-2000 Study Group], SLAC-REPRINT-1996-085.
19. D. Acosta *et al.* [CDF Collaboration], Phys. Rev. D **71** (2005) 051104.
20. The DØ Collaboration, DØnote 4375-CONF (2004).
21. See <http://cmsdoc.cern.ch/cms/PRS/results/susybsm/susybsm.html>.
22. W. L. van Neerven and E. B. Zijlstra, Nucl. Phys. B **382** (1992) 11 [Erratum-ibid. B **680** (2004) 513].
23. C. Anastasiou *et al.*, Phys. Rev. Lett. **91** (2003) 182002; Phys. Rev. D **69** (2004) 094008.
24. C. Balazs, J. W. Qiu and C. P. Yuan, Phys. Lett. B **355** (1995) 548.
25. S. Berge *et al.*, Phys. Rev. D **72** (2005) 033015.
26. A. D. Martin *et al.*, Eur. Phys. J. C **39** (2005) 155.
27. U. Baur *et al.*, Phys. Rev. D **65** (2002) 033007.
28. S. Dittmaier and M. Krämer, Phys. Rev. D **65** (2002) 073007; U. Baur and D. Wackerroth, Phys. Rev. D **70** (2004) 073015.
29. U. Baur, S. Keller and W. K. Sakumoto, Phys. Rev. D **57** (1998) 199.
30. P. Ciafaloni and D. Comelli, Phys. Lett. B **446** (1999) 278.
31. J. H. Kühn *et al.*, Nucl. Phys. B **616** (2001) 286 [Erratum-ibid. B **648** (2003) 455]; J. H. Kühn, A. A. Penin and V. A. Smirnov, Eur. Phys. J. C **17** (2000) 97; M. Beccaria *et al.*, Phys. Rev. D **61** (2000) 073005; J. H. Kühn and A. A. Penin, arXiv:hep-ph/9906545.
32. U. Baur and T. Stelzer, Phys. Rev. D **61** (2000) 073007.
33. W. Placzek and S. Jadach, Eur. Phys. J. C **29** (2003) 325.
34. C. M. Carloni Calame *et al.*, Eur. Phys. J. C **33** (2004) S665.
35. C. M. Carloni Calame *et al.*, JHEP **0505** (2005) 019.
36. Q. H. Cao and C. P. Yuan, Phys. Rev. Lett. **93** (2004) 042001.
37. K. Hagiwara *et al.*, Nucl. Phys. B **282** (1987) 253.
38. K. Hagiwara *et al.*, Phys. Lett. B **283** (1992) 353; Phys. Rev. D **48** (1993) 2182.
39. U. Baur and D. Zeppenfeld, Phys. Lett. B **201** (1988) 383.
40. The LEP Collaborations, LEPEWWG/TGC/2005-01.
41. See J. Ellison and J. Wudka, Ann. Rev. Nucl. Part. Sci. **48** (1998) 33 and references therein.
42. V. M. Abazov *et al.* [DØ Collaboration], Phys. Rev. Lett. **95** (2005) 141802.
43. J. Ohnemus and J. F. Owens, Phys. Rev. D **43** (1991) 3626; J. Ohnemus, Phys. Rev. D **44** (1991) 1403; Phys. Rev. D **44** (1991) 3477; Phys. Rev. D **47** (1993) 940; U. Baur, T. Han and J. Ohnemus, Phys. Rev. D **48** (1993) 5140; Phys. Rev. D **51** (1995) 3381; Phys. Rev. D **53** (1996) 1098; Phys. Rev. D **57** (1998) 2823; J. M. Campbell and R. K. Ellis, Phys. Rev. D **60** (1999) 113006; L. J. Dixon, Z. Kunszt and A. Signer, Nucl. Phys. B **531** (1998) 3; Phys. Rev. D **60** (1999) 114037; K. L. Adamson, D. de Florian and A. Signer, Phys. Rev. D **65** (2002) 094041; Phys. Rev. D **67** (2003) 034016.
44. E. Accomando, A. Denner and S. Pozzorini, Phys. Rev. D **65** (2002) 073003; E. Accomando, A. Denner and A. Kaiser, Nucl. Phys. B **706** (2005) 325; E. Accomando, A. Denner and C. Meier, arXiv:hep-ph/0509234; W. Hollik and C. Meier, Phys. Lett. B **590** (2004) 69.
45. M. Spira *et al.*, Nucl. Phys. B **453** (1995) 17.
46. R. V. Harlander and W. B. Kilgore, Phys. Rev. Lett. **88** (2002) 201801; C. Anastasiou and K. Melnikov, Nucl. Phys. B **646** (2002) 220; V. Ravindran, J. Smith and W. L. van Neerven, Nucl. Phys. B **665** (2003) 325.
47. C. Anastasiou, K. Melnikov and F. Petriello, arXiv:hep-ph/0501130.
48. U. Aglietti *et al.*, Phys. Lett. B **600** (2004) 57; G. Degrossi and F. Maltoni, Phys. Lett. B **600** (2004) 255.
49. T. Han, G. Valencia and S. Willenbrock, Phys. Rev. Lett. **69** (1992) 3274; T. Figy, C. Oleari and D. Zeppenfeld, Phys. Rev. D **68** (2003) 073005; E. L. Berger and J. Campbell, Phys. Rev. D **70** (2004) 073011.
50. W. Beenakker *et al.*, Nucl. Phys. B **653** (2003) 151; L. Reina, S. Dawson and D. Wackerroth, Phys. Rev. D **65** (2002) 053017; S. Dawson *et al.*, Phys. Rev. D **67** (2003) 071503; S. Dawson *et al.*, Phys. Rev. D **68** (2003) 034022.
51. M. Dührssen *et al.*, Phys. Rev. D **70** (2004) 113009 and references therein.
52. F. Gianotti *et al.*, Eur. Phys. J. C **39** (2005) 293.
53. U. Baur, T. Plehn and D. L. Rainwater, Phys. Rev. Lett. **89** (2002) 151801; Phys. Rev. D **67** (2003) 033003; Phys. Rev. D **68** (2003) 033001.
54. U. Baur, T. Plehn and D. L. Rainwater, Phys. Rev. D **69** (2004) 053004.